

Standardized extract of *Sanguisorba minor* attenuates injury in aging rat model *via* the Nrf2/HO-1 pathway

Farshad Mirzavi¹, Arezoo Rajabian^{2*}, Samaneh Boroumand-Noughabi^{3,4}, Azar Hosseini^{5,6},
Mohammad Taher Boroushaki^{5,6}, Sonita Hassanzadeh⁵

¹ Cardiovascular Diseases Research Center, Birjand University of Medical Sciences, Birjand, Iran,

² Department of Internal Medicine, Faculty of Medicine, Mashhad University of Medical Sciences, Mashhad, Iran,

³ Department of Pathology, Mashhad University of Medical Sciences, Mashhad, Iran,

⁴ Department of Hematology and Blood Banking, Faculty of Medicine, Mashhad University of Medical Sciences, Mashhad, Iran,

⁵ Department of Pharmacology, Faculty of Medicine, Mashhad University of Medical Sciences, Mashhad, Iran,

⁶ Pharmacological Research Center of Medicinal Plants, Mashhad University of Medical Sciences, Mashhad, Iran,

*Email: rajabianar@mums.ac.ir

Aging promotes damage to vulnerable organs like brain and liver. *Sanguisorba minor* has been traditionally used to cure various ailments. Few studies have reported pharmacological activities of this medicinal plant. This research aimed to investigate the effects of *Sanguisorba minor* extract (SME) on brain and liver injury in aging rats and identify the underlying mechanisms. The aging model was developed by subcutaneously injecting D-galactose and simultaneously treating them with SME. After biochemical and pathological assessments, mRNA expression levels of nuclear factor-erythroid factor 2-related factor 2 (Nrf2) and Nrf2-regulated gene, heme oxygenase-1 (HO-1), in the brain and liver tissues were determined. As a result, malondialdehyde and acetylcholinesterase levels were elevated while total thiol content and superoxide dismutase were reduced in the aging rats. Treatment with the extract remarkably attenuated oxidative injury and pathological changes in liver and brain tissues. Concomitantly, the extract up-regulated Nrf2 and HO-1 genes. Our findings exhibited SME may improve the aging-related brain and liver damage through the Nrf2-HO-1 pathway.

Key words: *Sanguisorba minor*, aging, D-galactose, liver function, neurodegeneration

INTRODUCTION

Aging is a gradual degenerative process characterized by the accumulation of molecular and cellular damage, leading to a wide range of age-related disorders including live failure and neurodegenerative diseases (Fulop et al., 2010; Campisi, 2013). D-galactose, a reducing sugar, naturally found in the body and in various foods (Azman et al., 2019) contributes to glucose metabolism. However, excess amounts of D-galactose were associated with the accumulation of aldose and hydroperoxide triggering the formation of reactive oxygen species (ROS) and decreasing endogenous antioxidant enzyme activity (Azman et al., 2019). There-

fore, it enhances oxidative stress in the brain and liver (Yu et al., 2015; Azman et al., 2019).

Oxidative stress plays a key role in the detrimental effects of aging (Chen et al., 2018; Azman et al., 2019). Exposure of body cells to high amounts of D-galactose provides conditions similar to aging (Shwe et al., 2018; Azman et al., 2019). Interestingly, the D-galactose-induced aging model has been extensively used to investigate a therapeutic approach for the prevention or alleviation of age-related conditions (Azman et al., 2019). Activation of nuclear factor-erythroid factor 2-related factor 2 (Nrf2) is an important response of body cells to oxidative injury (Schmidlin et al., 2019; Li et al., 2020a). Translocation of this transcription fac-

tor to the nucleus regulates gene expression of various antioxidant enzymes including heme oxygenase-1 (HO-1). A large number of medicinal plants and phytochemicals targeting Nrf2 were suggested to suppress oxidative injury-related disorders (Rajabian et al., 2019; Li et al., 2020a).

Sanguisorba minor (*S. minor*) belonging to the Rosaceae family that has been used in traditional medicine to cure diseases including bleeding, eczema, and diarrhea (Zhao et al., 2017). Recent evidence reported different biological activities of *S. minor* extracts including anti-inflammatory, antibacterial, antiviral, antioxidant, neuroprotective, and anticancer properties (Zhao et al., 2017; Cirovic et al., 2020; Finimundy et al., 2020). Moreover, the ethanol extract of *S. minor* was also found to suppress cyclooxygenase-1 (COX-1) and acetylcholinesterase (AChE) enzymes activity *in vitro* (Cirovic et al., 2020; Finimundy et al., 2020). Neuro-protective properties of *S. minor* against β -amyloid neurotoxicity were also manifested (Ferreira et al., 2006; Nguyen et al., 2008; Soodi et al., 2017; Akbari et al., 2019). Accordingly, this research aimed to investigate the effects of *S. minor* extract (SME) on brain and liver injury in aging rats and identify the underlying mechanisms.

METHODS

Chemicals

D-galactose, pyrogallol, acetylthiocholine iodide, phosphate-buffered saline (PBS), and 3-(dimethylthiazol-2-yl)-diphenyl tetrazolium (MTT) were purchased from Sigma-Aldrich (St. Louis, USA). DTNB (2,2'-dinitro-5,5'-dithiodibenzoic acid), trichloroacetic acid (TCA), thiobarbituric acid (TBA), hydrochloric acid (HCl), ethylenediamine tetra acetic acid disodium salt (Na₂EDTA), tris (hydroxymethyl) aminomethane (Trizma base), methanol, and dimethyl sulfoxide (DMSO) were obtained from Merck (Darmstadt, Germany).

Extract preparation of *S. minor* and standardization of the hydro-ethanolic extract

The fresh herb of *S. minor* with herbarium No. 45489 was collected from Ghoochan region, Khorasan Razavi province, Iran. The extraction was conducted as previously reported (Moradzadeh et al., 2019). In brief, the aerial parts of *S. minor* were dried under shade and powdered by a mixer grinder. The powder was macerated (50 g) in hydro-ethanolic solution (70%, v/v) for 48 h, under shaking, at 40°C. The suspension was then

filtered and completely dried under reduced pressure by means of rotary evaporation at 37°C. The resultant extract were kept at the refrigerator (-20°C).

High performance liquid chromatography (HPLC) system (Knauer, Berlin, Germany) apparatus was used to standardize the extract. Ellagic acid was used as the reference compound. The characteristic of chromatographic separation were as follow: a reverse-phase waters C18 analytical column (10×4.6 mm, 5 mm particle size), elution using a mixture composed of methanol-deionized water (20-100% v/v), the flow rate (for the injected extract) of 15 min, detection wavelength of 254 nm (Rajabian et al., 2016).

Animals and treatments

All treatments and maintenance of the animals were conducted in compliance with the National Institutes of Health Guidance for the Care and Use of Laboratory Animals and the Animal Ethics Committee of the Mashhad University of Medical Sciences (IR.MUMS.MEDICAL.REC.1399.738). A total of 40 male Wistar rats (weighted 200 ± 20 g) were acquired from the animal house of the Faculty of Medicine, Mashhad University of Medical Sciences (Mashhad, Iran). The rats were acclimatized and faced with standard conditions (room temperature: 24-25°C and on a 12 h light/12 h dark schedule). The animals had free access to food and water during the experiment. They were randomly divided into four groups (10 rats per group). The normal control group received saline 0.9% (subcutaneously injection) and tap water (oral gavage). D-galactose group received D-galactose (500 mg/kg, subcutaneously injection (Azman et al., 2019). In D-galactose-extract 50 and D-galactose-extract 100 groups, SME at doses of 50 and 100 mg/kg (oral gavage) and D-galactose were administrated (500 mg/kg, subcutaneously injection). To prepare the doses of 100, 200, and 400 mg/kg, the dried extract was dissolved in the tap water. All treatments were done for 10 consecutive weeks. After the treatments, the rats were sacrificed. Then, the blood samples were collected and the serum was separated. Meanwhile, the right hemisphere of the brain and parts of the liver were fixed in formalin solution (10%) for histological analysis. The other hemisphere of the brain and the residual liver tissues were stored at -80°C for biochemical assays.

Biochemical analysis

Serum alanine aminotransferase (ALT), aspartate aminotransferase (AST) activities were determined

colorimetrically by Autoanalyzer BT 3500 (Biotechnica, Italy) and Pars Azmun kit (Tehran, Iran).

Assessment of lipid peroxidation

The homogenates of the hippocampus (10% w/v) in ice-cold PBS (0.1 M, pH 7.4) were prepared and then centrifuged at 4°C, at 10000×g to separate the supernatants for further biochemical assessment.

In brief, to determine malondialdehyde (MDA) concentration, as the main product of lipid peroxidation, the homogenates (1 ml) were mixed with a solution containing TBA/TCA/HCL reagent (2 ml). Finally, the absorbance of the resultant thiobarbituric acid reactive substances was recorded at 412 nm spectrophotometrically (Hosseini et al., 2015).

Assay of total thiol content

Briefly, to assess the total thiol in the hippocampus and liver tissues, each sample (50 µl) was added to Tris-EDTA buffer (1 ml, pH=8.6) and the absorbance (at 240 nm) was recorded before and after adding of DTNB solution (10 mM) to each sample (Hosseini et al., 2015).

Assay of antioxidant enzyme activity

To assess SOD activity in the hippocampus, each sample (10 µl) was mixed with MTT and pyrogallol solution and then DMSO was added to solubilize the resultant color. One enzyme unit was defined as the amount of the SOD inhibiting the rate of pyrogallol auto-oxidation by 50%. The activity of SOD was expressed as unit per gram of tissue (Beheshti et al., 2021).

Estimation of AChE activity

To determine the AChE activity in the hippocampus, each sample (50 µl) was added to a solution (containing

PBS (pH 8), 0.1 ml DTNB (10 mM), and 0.02 ml acetylthiocholine iodide (75 mM). The changes in absorbance of the samples were measured at 412 nm during 10 min (Hosseini et al., 2015).

Quantitative realtime polymerase chain reaction (qRT-PCR)

Firstly, total RNA was extracted liver and hippocampus tissues using the RNA extraction kit (Pars Tous, Iran). NanoDrop 1000 (Thermo, Wilmington, USA) was used to assess the concentration and the resultant RNA purity followed by reverse transcription into cDNA using ExcelRT™ Reverse Transcription Kit II (SMOBIO, Taiwan). According to the manufacture's instruction, Light Cycler 96 Real-Time PCR System (Roche, Germany) with RealQ Plus 2x Master Mix Green (Ampliqon, Denmark) was used for qRT-PCR. The gene expression was normalized to GAPDH (glyceraldehyde-3-phosphate dehydrogenase) as an internal control gene, and fold change in genes expression levels was calculated with the $2^{-\Delta\Delta CT}$ method (Livak et al., 2001). The list of primer sequences is presented in the Table 1.

Histopathological examinations

The brain tissues were collected and quickly fixed in 10% buffered formalin. Afterward, the tissues were introduced to dehydration and inserting in paraffin. After that, hematoxylin and eosin (HE) were used for staining of the tissue sections of 5 µm. A Leica DMRB light microscope (India) equipped with a digital camera was used for imaging the histological paraffin sections was performed.

Statistical analysis

Statistical analyses were conducted by GraphPad Prism software 9.0 (GraphPad Software, La Jolla, CA, USA). The data were evaluated by one-way ANOVA followed by Tukey's *post hoc* multiple comparison test. The

Table 1. Primer sequence for qRT-PCR.

Gene name	Forward (5'→3')	Reverse (5'→3')	Product length (bp)
Nrf2	CTGTCAGCTACTCCAGGTTG	AAGCGACTCATGGTCATCTACA	113
HO-1	ATCGTGCTCGCATGAACACT	AGCTCCTCAACAGCTCAATGT	106
GAPDH	AGTGCCAGCCTCGTCTCAT	TGAACTTGCCGTGGGTAGAG	189

data were expressed as mean \pm SEM, and the differences were reported statistically significant, when they were less than 0.05, 0.01, and 0.001.

RESULTS

Effects of SME on hippocampal and hepatic tissues

According to the chromatographic pattern of the extract compared with that of the retention time of ellagic acid, as a standard, the estimated amount of ellagic acid in the extract (g) was 1.7% (Fig. 1).

Administration of D-galactose for 10 weeks led to a significant increase in MDA level in the hippocampus ($p<0.001$) and liver ($p<0.01$) compared with the control group. SME at doses 50 mg/kg and 100 mg/kg was able to reduce the MDA level in the hippocampus ($P<0.05$ and $P<0.01$) and liver ($P<0.05$ and $P<0.001$) compared with the D-galactose group (Fig. 2A, B). In addition, total thiol concentration (Fig. 2C, D) and SOD activity (Fig. 3A, B) in both liver and hippocampus were significantly reduced in the animals subjected to D-galactose toxicity ($p<0.001$ and $P<0.01$, respectively). Interestingly, both total thiol and SOD levels in the hippocampus ($p<0.001$) and liver ($p<0.01$) decreased. However, total thiol concentration significantly enhanced following treatment with SME in both liver ($p<0.05$ for both doses) and hippocampus ($p<0.01$ for 100 mg/kg). Treatment with SME

at both doses also enhanced the SOD activity in the liver ($p<0.05$ and $p<0.01$ for 50 and 100 mg/kg) and hippocampus ($p<0.05$) compared with the D-galactose group.

As shown in Fig. 3C, the activity of AChE significantly increased in the hippocampus of the animals-treated D-galactose in comparison with the control group ($p<0.001$). Treatment with SME at a dose of 100 mg/kg significantly lowered the enzyme activity in the hippocampus compared with the D-galactose group ($p<0.01$).

As shown in Fig. 3D, E the activity of AST and ALT significantly increased in the liver of the animals-treated D-galactose in comparison with the control group ($p<0.001$ and $p<0.01$, respectively). Treatment with SME at doses of 50 mg/kg ($p<0.01$) and 100 mg/kg ($p<0.01$ and $p<0.05$) significantly lowered activity of AST and ALT in the liver compared with D-galactose-group.

Effects of SME on the gene expression

As shown in Fig. 4, D-galactose treatment significantly down-regulated the gene expression levels of HO-1 and Nrf2 in the hippocampus and liver of the D-galactose group when compared with the normal group ($p<0.05$ - $p<0.01$). Treatment with SME significantly altered the gene expression of HO-1 and Nrf2. Both doses of SME resulted in a significant increase in the expression of HO-1 in the liver ($p<0.05$) and hippocampus tissues ($p<0.05$ - $p<0.01$). Moreover, the level

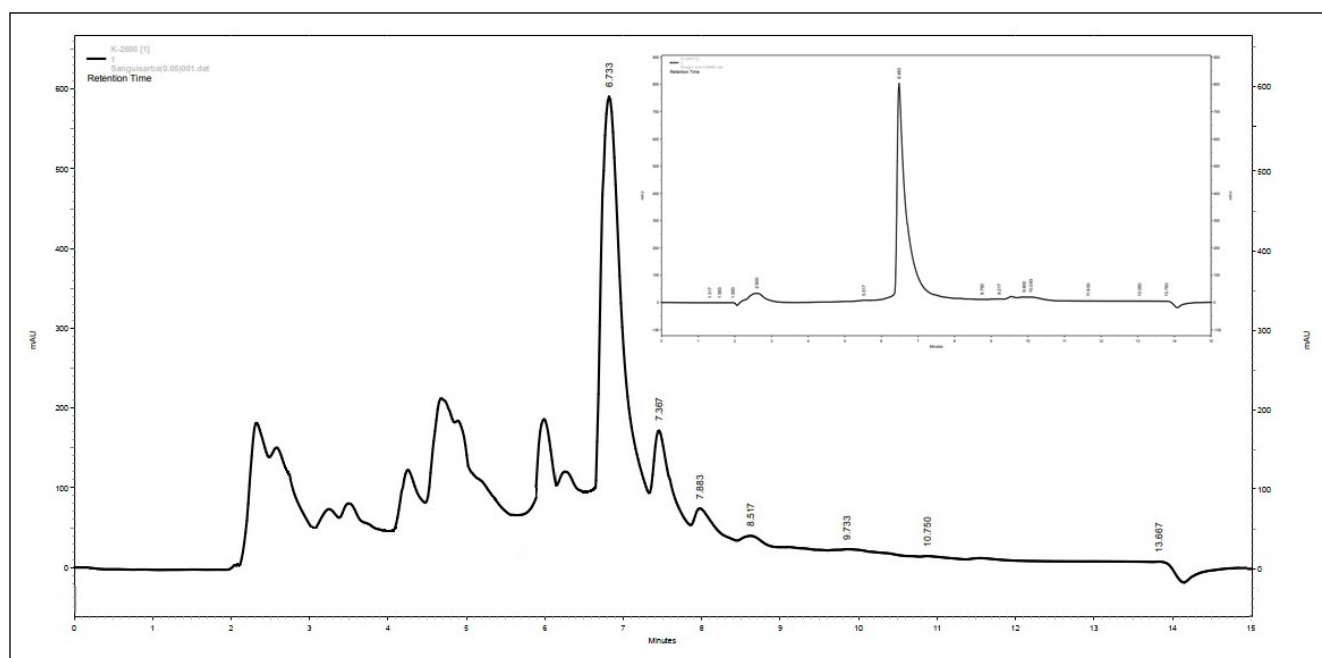


Fig. 1. The HPLC chromatogram of *S. minor* hydro-ethanolic extract and ellagic acid (retention time of 6.7 min).

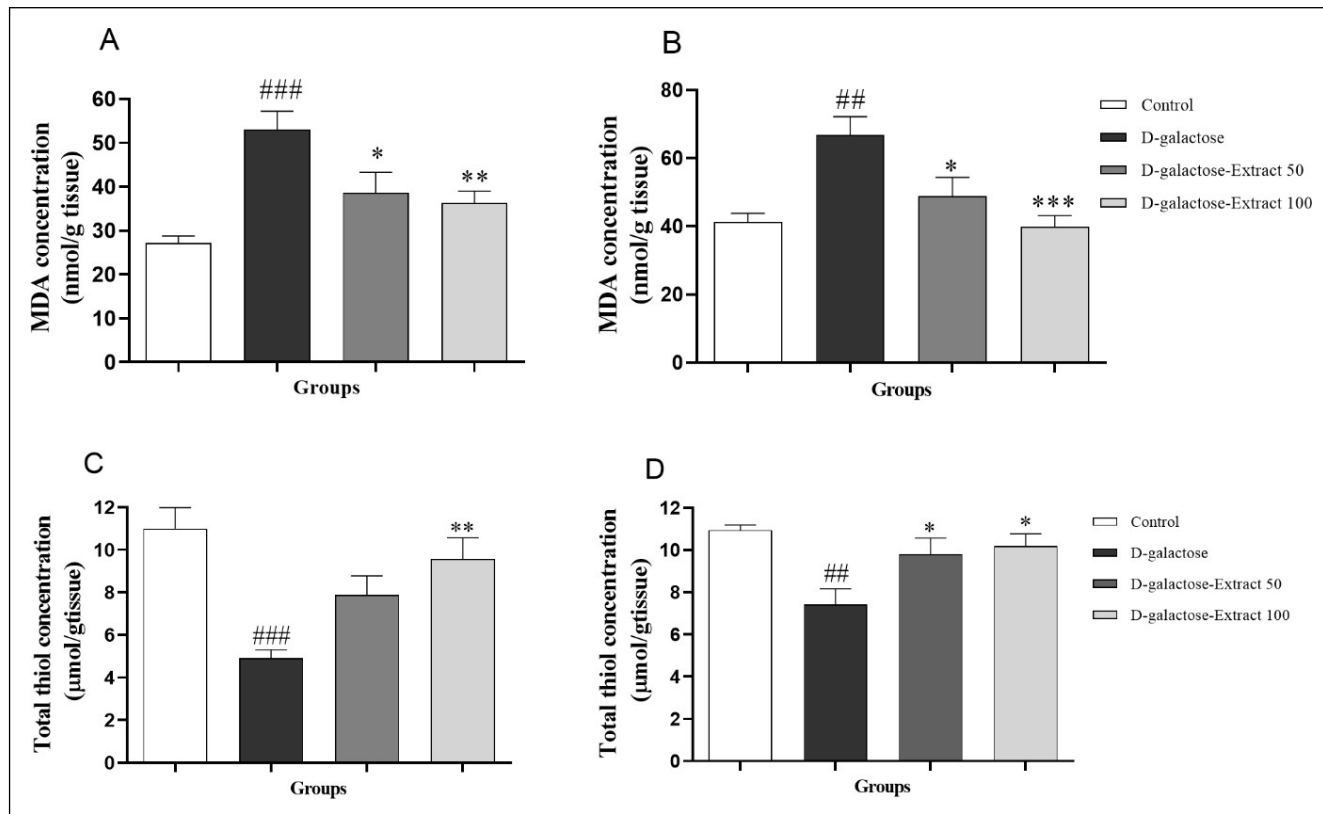


Fig. 2. Effect of *S. minor* on MDA (A: hippocampus, B: liver) and total thiol concentration (C: hippocampus, D: liver) in D-galactose-mediated aging. Data were expressed as mean \pm SEM (n=10). ^{##}P<0.01 and ^{###}P<0.001 compared to the control group, ^{*}P<0.05 and ^{**}p<0.01, and ^{***}P<0.001 compared to D-galactose group.

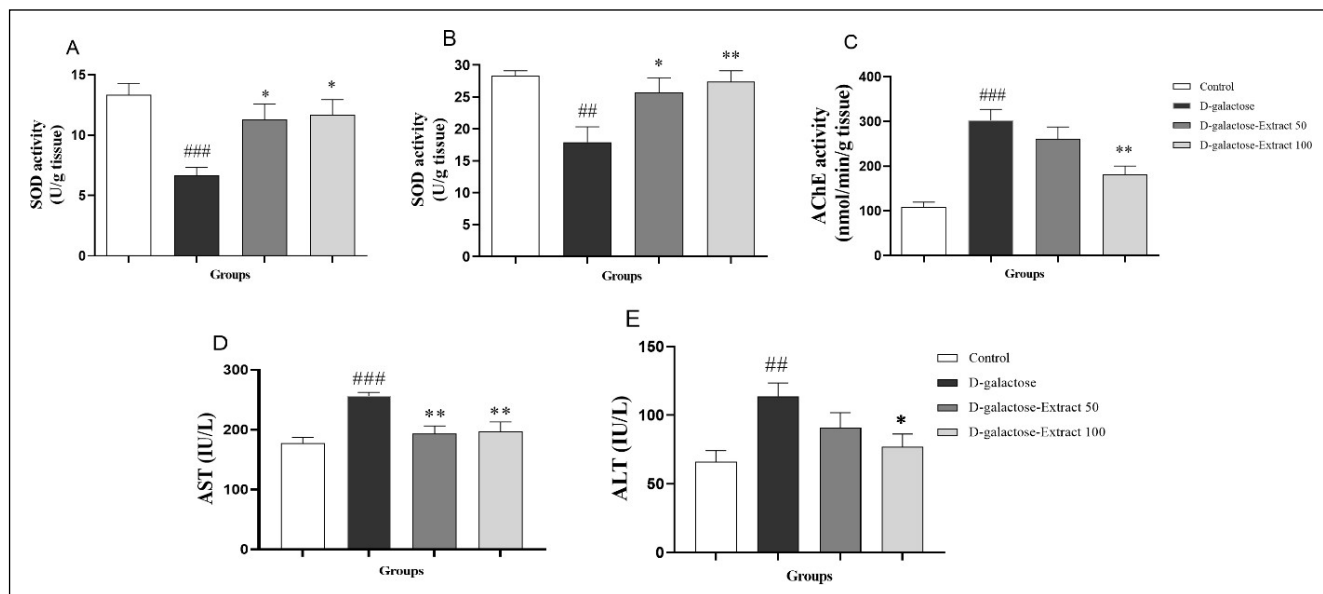


Fig. 3. Effect of *S. minor* on activity of SOD (A: hippocampus, B: liver), AChE (C: hippocampus), AST (D), and ALT (E) enzymes in D-galactose-mediated aging. Data were expressed as mean \pm SEM (n=10). ^{##}P<0.01 and ^{###}P<0.001 compared to the control group, ^{*}P<0.05 and ^{**}p<0.01, and ^{***}P<0.001 compared to D-galactose group.

of Nrf2 expression was significantly up-regulated in the liver ($p < 0.001$) and brain ($p < 0.05$) of SME groups. The levels HO-1 and Nrf2 gene expression in both tissues did not show any significant difference between low dose and high dose of SME ($p > 0.05$).

Histopathological observations

Histologic examination of the liver tissue in the control group demonstrated a normal architecture. Although, slight congestion was observed in some specimens from the control group. The rate of hepatocytes bi-nuclearity was low (about 2 to 3 per microscope high-power field (HPF)). The D-galactose-treated rats showed a normal architecture, mild congestion, and a high number of bi-nuclearity in the hepatocytes (about 8 to 9 per HPF). Examination of the liver in the extract-treated rats revealed a reduction in bi-nuclearity in the low dose-treated group (about 5 per HPF). Moreover, the rate of HPF in the high dose-treated group was found to be similar to the control group (2 to 3 per HPF). A number of degenerative changes including cell shrinkage, nuclear hyperchromasia as well as cytoplasmic hypereosino-

philia have been observed in the hippocampus neurons (CA3 part) of the brain specimens taken from the rats treated with D-galactose (Fig. 5). While the changes were resolved in the extract-treated groups (both low and high dose) and the neurons showed normal morphology similar to the sections from the control group.

DISCUSSION

Our study, for the first time, revealed the protective effects of SME on D-galactose-induced model of aging. As a result, administration of D-galactose led to morphological changes in liver and brain, and antioxidant system failure. However, SME probably activated the Nrf2-mediated pathway to counteract the deteriorative effects of D-galactose-induced aging.

Long-term exposure to high concentrations of D-galactose cause overproduction of free radicals and consequently defeat the anti-oxidative defense system (Sha et al., 2019). Regarding the key role of oxidative stress in the mechanisms of neuronal and liver injury induced by D-galactose (Chen et al., 2018), we measured oxidative stress markers in the brain and liver tissues.

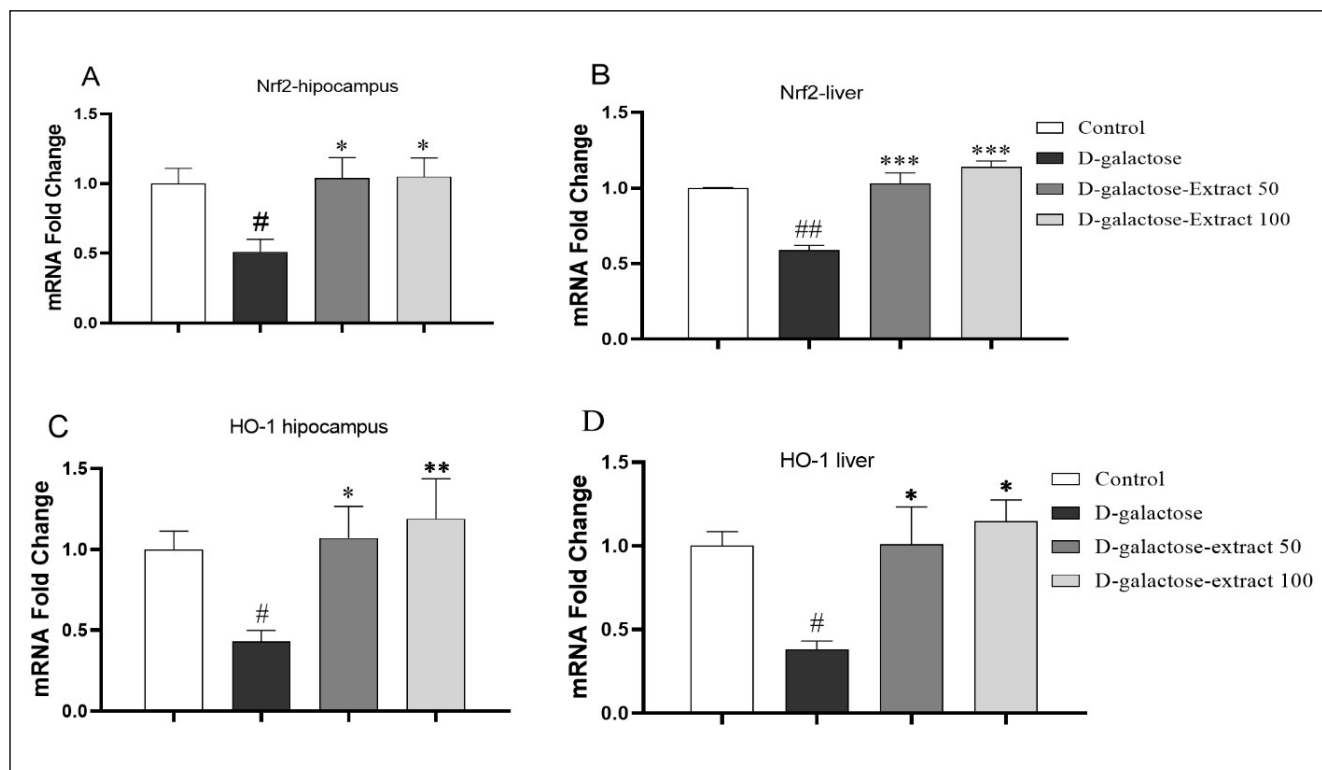


Fig. 4. Effect of *S. minor* on Nrf2 (A: hippocampus, B: liver) and HO-1 (C: hippocampus, D: liver) mRNA expression in D-galactose-mediated aging. Data were expressed as mean \pm SEM (n=6). * $P < 0.05$ and ** $P < 0.01$ compared to control group. * $P < 0.05$, ** $p < 0.01$, and *** $P < 0.001$ compared to D-galactose group.

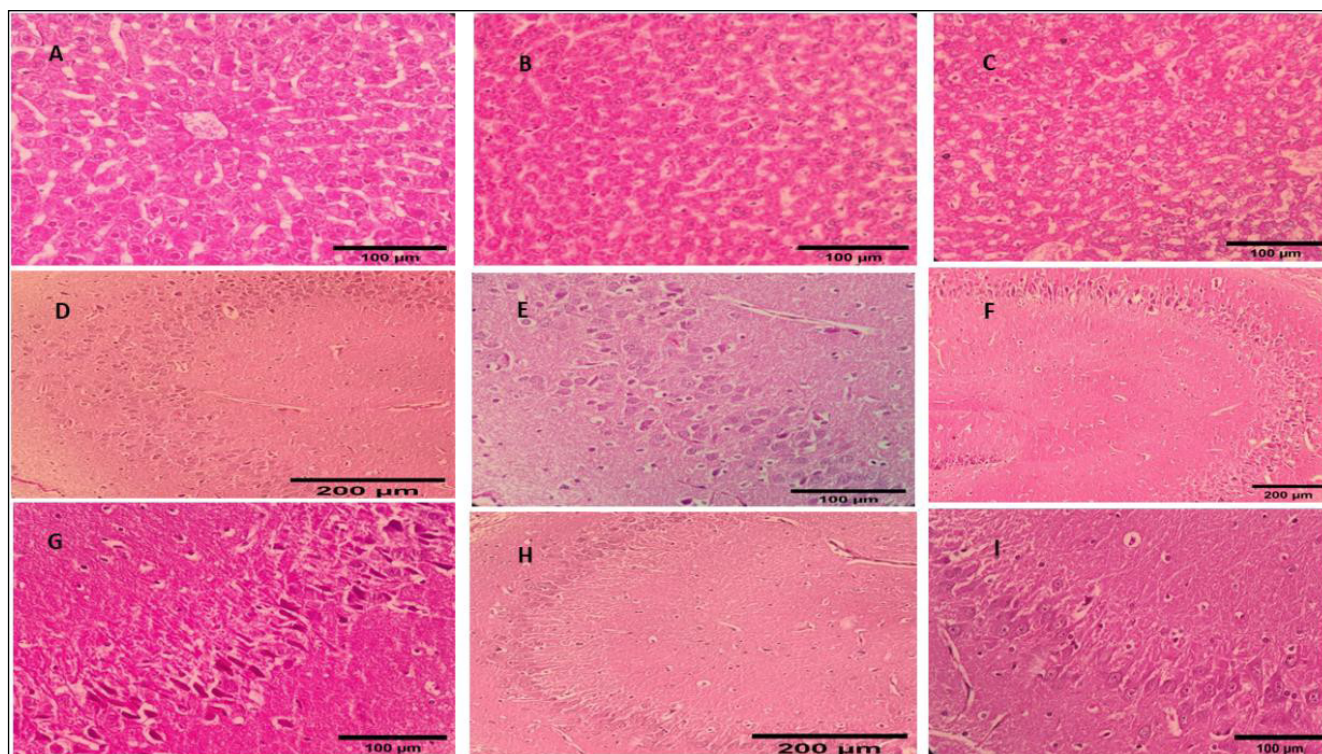


Fig. 5. Effect of *S. minor* on histopathological changes of liver and hippocampus tissues in the different experimental groups stained with hematoxylin and eosin (H&E). The sections of liver (A) and hippocampus (D and E) of control group showed normal appearance. The liver section of D-galactose group (B) showed a high number of bi-nucleated hepatocytes (black arrows) and the hippocampus sections of this group (F and G) showed nuclear hyperchromasia (black arrows) and cytoplasmic eosinophilia (white arrows). The liver section of 100 mg/kg extract and D-galactose group (C) showed a lowered number of bi-nucleated hepatocytes (black arrows) and the hippocampus sections of this group (H and I) showed normal appearance.

As our data revealed, D-galactose elevated MDA, a major oxidative injury product, while suppressed thiol level and SOD activity in the brain and liver tissues. These results were consistent with the previous investigations which showed that injection of D-galactose is associated with oxidative injury (Chen et al., 2018; Sha et al., 2019). Rat's liver and hippocampus were found to be two susceptible organs to injury induced by D-galactose (Chen et al., 2018; Sha et al., 2019).

The accumulation of D-galactose metabolites alters cell morphology, leading to neurodegeneration and hepatocellular injury. Free radicals formed during D-galactose metabolism also promote the aging progression (Chen et al., 2018; Sha et al., 2019). D-galactose overload impairs organ functions including the brain and liver. It was found that exposure to the high dose of D-galactose was accompanied by increased AChE in the brain (Wei et al., 2017; Sha et al., 2019) as well as ALT and AST activity in the liver (Chen et al., 2018). Consistently, our study showed that D-galactose injection resulted in an increase in activity of AChE in brain as well as AST and ALT in the liver. Meanwhile, D-galactose induced morphological changes in both

the liver and brain. Therefore, our results may also be a confirmation of the proposed important role of oxidative stress in aging mediated by D-galactose. Hence, the antioxidant compounds may modulate redox status in D-galactose injury (Chen et al., 2018; Sha et al., 2019; Li et al., 2020b).

Previous evidence indicated that *S. minor* contains phytochemicals, which can remove reactive oxygen species such as hydroxyl radical ($\cdot\text{OH}$) as well as it has shown the ability for scavenging 1,1-diphenyl-2-picrylhydrazyl (DPPH) free radicals (Zhao et al., 2017; Akbari et al., 2019; Cirovic et al., 2020). Moreover, in a study conducted by Ferreira et al. (2006), the ethanol extract and essential oil of *S. minor* exhibited the anti-oxidant and AChE inhibitory effects. In the same context, *S. minor* showed neuroprotective activities against oxidative injury induced by β -amyloid in cultured cerebellar granule neurons (Soodi et al., 2017; Akbari et al., 2019). AChE inhibitory properties of this plant have been proposed to be involved in the neuroprotective effect of *S. minor* (Akbari et al., 2019).

A number of phenolic and flavonoid compounds present in *S. minor* extract are responsible for its an-

tioxidant and neuroprotective functions (Akbari et al., 2019; Cirovic et al., 2020). Interestingly, the phytochemicals such as quercetin and ellagic acid were found to suppress AChE activity (Szwajgier, 2013; Ademosun et al., 2016; Khan et al., 2018; Dornelles et al., 2020). Hence, they were proposed to enhance cholinergic function of brain (Khan et al., 2018; Dornelles et al., 2020).

The findings obtained from the present study confirmed the previous results. Accordingly, SME protected against oxidative stress as well as alleviated concomitant histopathological changes induced by D-galactose in the liver and brain. Additionally, SME reversed increased AST and ALT activities which can be correlated with liver dysfunction in the presence of D-galactose. Therefore, the antioxidant effects of SME against brain and liver damage, at least partly, were attributed to its protection against oxidative stress. The data propose the capacity of SME to attenuate age-associated oxidative stress. When the body cells expose to oxidative conditions, Nrf2/HO-1 signaling pathway, as an important antioxidant pathway, is activated. Activation of Nrf2 up-regulates gene expression of antioxidant and phase II detoxification enzymes including HO-1, SOD (Li et al., 2020a). As previously illustrated, exposure to D-galactose reduces Nrf2 activation and translocation to the nucleus (Azman et al., 2019; Schmidlin et al., 2019).

Our findings demonstrated that Nrf2/HO-1 pathway is involved in the D-galactose-induced aging process, and the extract may induce a protective effect by activating Nrf2 pathway and enhancing the expression of its downstream antioxidants, such as HO-1 and SOD.

CONCLUSION

Our results also indicated that SME exerts antioxidant, hepato-protective, and anti-neurodegenerative effects against D-galactose aging. Activation of the Nrf2 pathway at least in part contributes to the protection against D-galactose-induced aging in rats. This pathway may be helpful for approaching the issues associated with anti-ageing in the future. Moreover, our findings indicating the neuroprotective effects of *S. minor* would encourage and facilitate further research on development of more effective anti-aging agents.

ACKNOWLEDGEMENTS

This study was originated from MD project of Sonita Hassanzadeh. The authors appreciate the Vice Chancel-

lor for Research and Technology, Mashhad University of Medical Sciences for financial support (Grant No. 990936).

This project was financially supported by Vice Chancellery for Research and Technology, Mashhad University of Medical Sciences for financial support (Grant No. 990936).

REFERENCES

- Ademosun AO, Oboh G, Bello F, Ayeni PO (2016) Antioxidative properties and effect of quercetin and its glycosylated form (Rutin) on acetylcholinesterase and butyrylcholinesterase activities. *J Evid Based Complementary Altern Med* 21 : NP11–NP17.
- Akbari S, Soodi M, Hajimehdipoor H, Ataei N (2019) Protective effects of *Sanguisorba minor* and *Ferulago angulata* total extracts against beta-amyloid induced cytotoxicity and oxidative stress in cultured cerebellar granule neurons. *J Herbmed Pharmacol* 8: 248–255.
- Azman KF, Zakaria R (2019) D-galactose-induced accelerated aging model: an overview. *Biogerontology* 20: 763–782.
- Beheshti F, Akbari HR, Baghchehghi Y, Mansouritorghabeh F, Mortazavi Sani SS, Hosseini M (2021) Beneficial effects of angiotensin converting enzyme inhibition on scopolamine-induced learning and memory impairment in rats, the roles of brain-derived neurotrophic factor, nitric oxide and neuroinflammation. *Clin Exp Hypertens* 43: 1–11.
- Campisi J (2013) Aging, cellular senescence, and cancer. *Annu Rev Physiol* 75: 685–705.
- Chen P, Chen F, Zhou B (2018) Antioxidative, anti-inflammatory and anti-apoptotic effects of ellagic acid in liver and brain of rats treated by D-galactose. *Sci Rep* 8: 1–10.
- Cirovic T, Barjaktarevic A, Ninkovic M, Bauer R, Nikles S, Brankovic S, et al. (2020) Biological activities of *sanguisorba minor* L extracts in vitro and in vivo evaluations. *Acta Pol Pharm* 77: 745–758.
- Dornelles GL, de Oliveira JS, de Almeida EJR, Mello CBE, Rodrigues BR, da Silva CB, et al (2020) Ellagic acid inhibits neuroinflammation and cognitive impairment induced by lipopolysaccharides. *Neurochem Res* 45: 2456–2473.
- Ferreira A, Proença C, Serralheiro M, Araujo M (2006) The in vitro screening for acetylcholinesterase inhibition and antioxidant activity of medicinal plants from Portugal. *J Ethnopharmacol* 108: 31–37.
- Finimundy TC, Karkanis A, Fernandes Â, Petropoulos SA, Calheta R, Petrović J, et al. (2020) Bioactive properties of *Sanguisorba minor* L cultivated in central Greece under different fertilization regimes. *Food Chem* 327: 127043.
- Fulop T, Larbi A, Witkowski JM, McElhaney J, Loeb M, Mitnitski A, et al. (2010) Aging, frailty and age-related diseases. *Biogerontology* 11: 547–563.
- Hosseini M, Mohammadpour T, Karami R, Rajaei Z, Sadeghnia HR, Soukhtanloo M (2015) Effects of the hydro-alcoholic extract of *Nigella sativa* on scopolamine-induced spatial memory impairment in rats and its possible mechanism. *Chin J Integr Med* 21: 438–444.
- Khan H, Amin S, Kamal MA, Patel S (2018) Flavonoids as acetylcholinesterase inhibitors: Current therapeutic standing and future prospects. *Biomed Pharmacother* 101: 860–870.
- Li B, Nasser M, Masood M, Adlat S, Huang Y, Yang B, et al. (2020a) Efficiency of traditional Chinese medicine targeting the Nrf2/HO-1 signaling pathway. *Biomed Pharmacother* 126: 110074.
- Li T, Wu CE, Meng X, Fan G, Cao Y, Ying R, et al. (2020b) Structural characterization and antioxidant activity of a glycoprotein isolated from *Camellia oleifera* Abel seeds against D-galactose-induced oxidative stress in mice. *J Funct Foods* 64: 103594.

- Livak KJ, Schmittgen TD (2001) Analysis of relative gene expression data using real-time quantitative PCR and the 2- $\Delta\Delta$ CT method. *Methods* 25: 402–408.
- Moradzadeh M, Rajabian A, Aghaei A, Hosseini A, Sadeghnia HR (2019) Rheum turkestanicum induced apoptosis through ROS without a differential effect on human leukemic cells. *Jundishapur J Nat Pharm Prod* 14: e12198.
- Nguyen TTH, Cho SO, Ban JY, Kim JY, Ju HS, Koh SB, et al. (2008) Neuro-protective effect of Sanguisorbae radix against oxidative stress-induced brain damage: in vitro and in vivo. *Biol Pharm Bull* 31: 2028–2035.
- Rajabian A, Boroushaki MT, Hayatdavoudi P, Sadeghnia HR (2016) Boswellia serrata protects against glutamate-induced oxidative stress and apoptosis in PC12 and N2a cells. *DNA Cell Biol* 35: 666–679.
- Rajabian A, Hosseini A, Hosseini M, Sadeghnia HR (2019) A review of potential efficacy of Saffron (Crocus sativus L) in cognitive dysfunction and seizures. *Prev Nutr Food Sci* 24: 363.
- Schmidlin CJ, Dodson MB, Madhavan L, Zhang DD (2019) Redox regulation by NRF2 in aging and disease. *Free Radic Biol Med* 134: 702–707.
- Sha JY, Zhou YD, Yang JY, Leng J, Li JH, Hu JN, et al. (2019) Maltol (3-hydroxy-2-methyl-4-pyrone) slows D-galactose-induced brain aging process by damping the Nrf2/HO-1-mediated oxidative stress in mice. *J Agric Food Chem* 67: 10342–10351.
- Shwe T, Pratchayasakul W, Chattipakorn N, Chattipakorn SC (2018) Role of D-galactose-induced brain aging and its potential used for therapeutic interventions. *Exp Gerontol* 101: 13–36.
- Soodi M, Hajimehdipoor H, Akbari S, Ataei N (2017) Screening seven Iranian medicinal plants for protective effects against β -Amyloid-induced cytotoxicity in cultured cerebellar granule neurons. *Res J Pharmacogn* 4: 15–22.
- Szwajgier D (2013) Anticholinesterase activity of phenolic acids and their derivatives. *Z Naturforsch C* 68: 125–132.
- Wei H, Gao Z, Zheng L, Zhang C, Liu Z, Yang Y, et al. (2017) Protective effects of fucoidan on A β 25–35 and d-Gal-induced neurotoxicity in PC12 cells and d-Gal-induced cognitive dysfunction in mice. *Mar Drugs* 15: 77.
- Yu Y, Bai F, Liu Y, Yang Y, Yuan Q, Zou D, et al. (2015) Fibroblast growth factor (FGF21) protects mouse liver against D-galactose-induced oxidative stress and apoptosis via activating Nrf2 and PI3K/Akt pathways. *Mol Cell Biochem* 403: 287–299.
- Zhao Z, He X, Zhang Q, Wei X, Huang L, Fang JC, et al. (2017) Traditional uses, chemical constituents and biological activities of plants from the genus Sanguisorba L. *Am J Chinese Med* 45: 199–224.